

Abstract

Atmospheric loadings of secondary organic aerosols (SOA) are significantly under-predicted by climate models. In these models, SOA particles are assumed liquid-like droplets at equilibrium with the gas-phase. In sharp contrast, our recent laboratory and field measurements show that SOA particles are non-rigid, highly viscous, spherical, quasi-solids, and do not behave like liquid droplets. They evaporate at rates much lower than predicted by models, and are consequently not at equilibrium with the gas phase. In addition, our data show that SOA particles trap hydrophobic organics, whose presence further reduces evaporation rates, and that aging these particles nearly stops evaporation. Measurements of the evaporation kinetics of ambient SOA particles under vapor-free conditions at room temperature showed that less than 20 % of particle mass evaporates in 4 h.

In this study, we examine, for the first time, these groundbreaking observations to present a new, experimentally based picture of the phase and evaporation behavior of SOA particles. We conclude that to first order SOA can be reasonably approximated to be non-evaporating. We use a simplified approach to investigate the implications of this near-irreversible gas-particle partitioning behavior in a box model and a 3-D chemical transport model, both of which, for the first time, include multi-generational gas-phase chemistry with functionalization and fragmentation reactions, and compare them to traditional reversible partitioning models. Results indicate that the revised irreversible partitioning approach yields slightly higher SOA loadings than traditional reversible partitioning approach when functionalization reactions, pushing SOA species to lower volatility bins are dominant. However, when fragmentation reactions play a major role, the revised irreversible partitioning approach predicts significantly higher SOA than the traditional approach. In addition to irreversibility, functionalization, and fragmentation, we explore the utility of lower activity coefficient to account for complex molecular interactions within particles and show that this approach predicts considerably higher SOA loadings. Using the 3-D Weather Research and Forecasting (WRF)

Reformulating the atmospheric lifecycle of SOA

M. Shrivastava et al.

Title Page

Abstract

Introduction

Conclusions

References

Tables

Figures

⏪

⏩

◀

▶

Back

Close

Full Screen / Esc

Printer-friendly Version

Interactive Discussion



model, coupled with Chemistry (WRF-Chem) modeling example of the Mexico City region, we demonstrate that when fragmentation is taken into account, irreversible partitioning increases predicted SOA loadings and lifetimes significantly compared to traditional models. When lower activity coefficient is also included, predicted SOA loadings in the Mexico City plateau increase by more than a factor of 3.

1 Introduction

Some of the largest uncertainties in modeling anthropogenic influences on climate involve the effects of atmospheric aerosols on radiation and on clouds as shown by Fig. 2.20 in chapter 2 of the IPCC 2007 report (Forster et al., 2007). Field measurements of atmospheric aerosol composition find that more than 50 % of the dry particles mass is organic aerosol (OA), of which secondary organic aerosol (SOA) is the dominant component. Compared to current model predictions, SOA loadings measured in the atmosphere are significantly higher (de Gouw et al., 2005; Robinson et al., 2007; Zhang et al., 2007; Heald et al., 2005; Volkamer et al., 2006). Despite intense ongoing research efforts, the large gap between models and observations remains (Goldstein and Galbally, 2007).

An extensive recent review on SOA formation, properties, and impact by Hallquist et al. (2009) notes that “The chemical and physical processes associated with SOA formation are complex and varied, and, despite considerable progress in recent years, a quantitative and predictive understanding of SOA formation does not exist and therefore represents a major research challenge in atmospheric science”. This prevailing conclusion is also reflected by other studies (Kroll and Seinfeld, 2008; Pöschl, 2005). In the present work, we introduce new experimental observations showing fundamental problems in current process-level understanding of SOA with tremendous implications on predictive abilities of aerosol models.

For the past two decades, temporal evolution of SOA has been modeled using the absorptive partitioning theory, which requires that SOA species reversibly partition

Reformulating the atmospheric lifecycle of SOA

M. Shrivastava et al.

Title Page

Abstract

Introduction

Conclusions

References

Tables

Figures

◀

▶

◀

▶

Back

Close

Full Screen / Esc

Printer-friendly Version

Interactive Discussion



Reformulating the atmospheric lifecycle of SOA

M. Shrivastava et al.

Title Page

Abstract

Introduction

Conclusions

References

Tables

Figures

⏪

⏩

◀

▶

Back

Close

Full Screen / Esc

Printer-friendly Version

Interactive Discussion



between gas and particle phases according to their sub-cooled liquid vapor pressures adjusted by Raoult's law (Donahue et al., 2006; Odum et al., 1996; Pankow, 1994). In addition, regional and global Chemical Transport Models represent SOA using empirical fits to smog chamber data, and often assume that thermodynamic equilibrium between gas and particle phase organics is achieved instantaneously (Chung and Seinfeld, 2002; Heald et al., 2005; Robinson et al., 2007). However, recent experimental findings from several studies provide substantial evidence suggesting that reversible absorptive gas-particle partitioning used to represent SOA behavior in the atmosphere needs to be reconsidered (Cappa and Wilson, 2011; Grieshop et al., 2007; Stanier et al., 2007; Vaden et al., 2010, 2011a; Virtanen et al., 2010; Zelenyuk et al., 2010).

The phase and morphology of SOA plays a very important role in deciding the particle phase dynamics (Molina et al., 1996; Ravishankara, 1997). Since diffusion rates within solid phase of a given species are several orders of magnitude lower than corresponding liquid phase (Ravishankara, 1997), particle phase dynamics in a diffusion-limited solid phase are subject to significantly greater mass-transfer limitations compared to liquids. A recent modeling study showed how changes in diffusivity altered by oligomerization may explain evolution of chemical loss rates in ageing amorphous semi-solid or glassy atmospheric aerosols (Pfrang et al., (2011). It is important to note that while considerable effort has been directed towards understanding the chemical-pathways for SOA formation (Kroll and Seinfeld, 2008), the physical and chemical morphology of SOA has not been extensively evaluated (Hallquist et al., 2009).

Gas-particle partitioning models assume that SOA particles are spherical liquid droplets in equilibrium with the gas-phase (Hallquist et al., 2009; Jimenez et al., 2009; Pankow, 1994). However, a number of recent studies have brought into question these fundamental assumptions used in current SOA models (Salcedo et al., 2006, 2007; Song et al., 2007; Vaden et al., 2010, 2011a; Virtanen et al., 2010). High SOA-content particles characterized by the Aerosol Mass Spectrometer (AMS) in Mexico City were measured to be aspherical and bounced from AMS vaporizer like sulfate particles, indicating that they may be solid (Salcedo et al., 2006, 2007). Similarly, Virtanen et al.,

Reformulating the atmospheric lifecycle of SOA

M. Shrivastava et al.

Title Page

Abstract

Introduction

Conclusions

References

Tables

Figures

⏪

⏩

◀

▶

Back

Close

Full Screen / Esc

Printer-friendly Version

Interactive Discussion



(2010) showed that SOA particles bounce from the electrical low-pressure impactor with a probability even higher than that of dry ammonium sulfate particles. They concluded that SOA particles are either amorphous solids or in glassy state. In contrast, Bahreini et al. (2005) observed significant increase in the AMS collection efficiency of sulfate particles once they became coated with SOA and suggested that the laboratory-generated SOA formed in reactions of cycloalkene ozonolysis are in liquid phase.

Using our single particle mass spectrometer, SPLAT II, we showed that α -pinene SOA particles are spherical and measured their density under a range of conditions with high precision (Vaden et al., 2010, 2011a, b; Zelenyuk et al., 2008). In addition, we characterized the shape and density of ambient SOA mixed with a small amount of sulfate and found these particles to be spherical (Vaden et al., 2011a).

Measurements by Song et al. (2007) cast doubt on the assumption of well-mixed liquid organic aerosol composed of hydrophilic SOA and hydrophobic organics. In Vaden et al. (2010), we describe experiments, in which we generated layered particles with liquid hydrophobic organic cores coated with α -pinene SOA, and particles of the opposite morphology, with SOA at the core and liquid hydrophobic organic on the surface, and demonstrated that both particle types remain stable for many hours. We concluded that diffusion through SOA must be extremely slow.

Previous measurements characterized volatility of SOA particles varying either dilution or residence time in flow tubes with short residence timescales ~seconds to minutes (Grieshop et al., 2007; Stanier et al., 2007). The observed slow evaporation were thought to be the manifestation of the fact that reversible thermodynamic equilibrium was not achieved due to the short “experimental timescales”, but would be achieved on sufficiently-short timescales to be irrelevant under atmospheric conditions. For the first time, in Vaden et al. (2011a), we used highly sensitive measurements at room temperature and atmospherically relevant (>24 h) timescales to show that SOA particles evaporate orders of magnitude slower than predicted by models, and are not in equilibrium with gas phase in the atmosphere, due to many complex physical and chemical processes which have not been thoroughly investigated so far.

In addition, we concluded that our observation, in these studies, of size-independent evaporation kinetics implied that SOA cannot be liquid droplets. Vaden et al. (2011a) also showed that diffusion of semi-volatile organic species, like pyrene, through SOA is extremely slow, providing direct evidence that SOA is highly viscous. Cappa and Wilson (2011) measured the evaporation kinetics of SOA as a function of temperature and found evaporation rates much slower than expected. Moreover, based on their mass spectral data they concluded that SOA must be highly viscous, citing Virtanen et al. (2010) and Vaden et al. (2011a) in support of their conclusion. Cappa and Wilson (2011) suggested that if ambient OA acted as a glassy substance with slow diffusion, then SOA properties derived on the basis of absorptive partitioning theory would not be physically and chemically meaningful and proposed a new sequential partitioning SOA model, in which the particles harden into a “non-absorbing” core during formation. Similarly, Virtanen et al. (2010) called for a rethinking of the “traditional views of the kinetics and thermodynamics of SOA formation and transformation in the atmosphere and to their implications for air quality and climate.” In addition, Kroll and Seinfeld (2008) reviewed multiple lines of evidence from various laboratory and ambient studies showing oligomer formation (species of low volatility and high molecular weight). Halquist et al. (2009) suggested that viscosity of organic particles could be enhanced by oligomerization, which may also inhibit particle-phase reactions.

Considered together, these findings cast doubt on the assumption that SOA particles and vapors maintain equilibrium by rapid reversible partitioning. However, to-date they have been ignored by SOA models. Below we present analysis of our recent data on SOA size, composition, shape, morphology, phase, viscosity, and evaporation rates to develop a more complete picture of SOA particles. Multi-dimensional single particle characterization, in which all measured particle properties have to agree with aerosol process models, is a fundamental guiding principle of our research. We show that SOA particles are highly viscous quasi-solids, but are not rigid. Our observations of extremely slow evaporation rates even under vapor-free conditions at room temperature suggest that to first degree SOA particles can be assumed non-evaporating in

Reformulating the atmospheric lifecycle of SOA

M. Shrivastava et al.

Title Page

Abstract

Introduction

Conclusions

References

Tables

Figures

◀

▶

◀

▶

Back

Close

Full Screen / Esc

Printer-friendly Version

Interactive Discussion



Reformulating the atmospheric lifecycle of SOA

M. Shrivastava et al.

Title Page

Abstract

Introduction

Conclusions

References

Tables

Figures

◀

▶

◀

▶

Back

Close

Full Screen / Esc

Printer-friendly Version

Interactive Discussion



the atmosphere (i.e. irreversibly partitioned to particle phase). We explore the implications of non-evaporating SOA that is not in equilibrium with the gas-phase and assess the utility of mass accommodation coefficients to impose kinetic constraints on SOA formation and evaporation. Then, a box-modeling framework is used to compare the previous approach that assumes pseudo-ideal solution and reversible gas-particle partitioning based on Raoult's law, to our revised approach with irreversible partitioning and lower activity coefficient.

Moreover, current SOA models assume that oxidation reactions produce lower volatility compounds with 100% yield due to functionalization reactions (Robinson et al., 2007). Recent studies have shown that fragmentation reactions that produce higher volatility organic species are very important and need to be included in models (Jimenez et al., 2009; Kroll et al., 2011). We introduce fragmentation reactions in the box model and find that the differences between the irreversible and reversible partitioning approaches strongly depend on the relative importance of functionalization and fragmentation reactions. Using the 3-D Weather Research and Forecasting model coupled with chemistry (WRF-Chem) for Mexico City, we show that the new irreversible SOA picture and modeling approach leads to SOA loadings significantly higher than those predicted by current models.

2 An experimentally driven picture of SOA

2.1 SOA shape, morphology, phase, and viscosity

We have previously shown that laboratory generated α -pinene SOA particles are spherical and that their density is between 1.19 and 1.21 g cm⁻³, depending on reaction conditions (Vaden et al., 2010, 2011a, b; Zelenyuk et al., 2008). Recently, we extended the measurements of shape and density to characterize SOA particles produced from a range of precursors, and found all of them to be spherical. Similar measurements on ambient particles composed of SOA mixed with a small amount of sulfate show that

these particles were spherical with density of $1.32 \pm 0.02 \text{ g cm}^{-3}$ (Vaden et al., 2011a).

In recent SOA morphology study by Vaden et al. (2010), we produced α -pinene SOA in the presence of seed particles composed of dioctyl phthalate (DOP), a hydrophobic liquid organic, and showed that SOA is not soluble in DOP and that the resultant mixed particles had a layered structure with DOP core and SOA coating. In subsequent experiments, we generated pure SOA particles, by homogeneous nucleation, and coated these particles with DOP. These particles were also shown to be layered, with SOA at the core and a DOP coating. The fact that mixed SOA/DOP particles with two reverse morphologies were found to be stable for many hours indicates that diffusion through SOA must be very slow. Similarly, we recently found that pyrene, a solid poly aromatic hydrocarbon (PAH), does not dissolve in pure α -pinene SOA and forms instead a localized nodule on top of the SOA particle.

In Vaden et al. (2011a) we presented extensive measurements of the room temperature evaporation kinetics of size-selected SOA particles and showed that evaporation rates are significantly slower than expected. Based on this observation, we concluded that SOA could not maintain equilibrium with the gas phase by evaporation as predicted by models. In addition, we found that the evaporative SOA mass loss rate is nearly particle size independent, which is in sharp contrast with the expected behavior of liquid droplets. Furthermore, we showed that diffusion rates within SOA particles are extremely slow, and concluded that SOA must be highly viscous and cannot be a "liquid-like" substance Vaden et al. (2011a).

Virtanen et al. (2010) measured the bouncing probabilities of SOA particles and concluded that these particles cannot be liquids. Cappa and Wilson (2011) characterized the evaporation behavior of α -pinene SOA in a thermodenuder and reported that the SOA mass spectra do not change with increasing temperature, i.e. increasing SOA evaporated fraction. They concluded that these particles must be highly viscous, perhaps glassy, to explain their findings. In Vaden et al. (2011a) we reported small changes in mass spectral intensity of SOA with evaporation. We found that at short evaporation time (few minutes) the intensity of the peak at $m/z = 201$ decreased and

Reformulating the atmospheric lifecycle of SOA

M. Shrivastava et al.

Title Page

Abstract

Introduction

Conclusions

References

Tables

Figures

◀

▶

◀

▶

Back

Close

Full Screen / Esc

Printer-friendly Version

Interactive Discussion



at longer times the relative intensity of peaks at higher m/z slightly increased. Similarly, for ambient SOA particles we found that a significant fraction of the mass-spectral intensity of the peak at $m/z = 44$ and 73 decreased within a few evaporation minutes and concluded that it is due to the evaporation of a compound on the particle surface.

5 However, compared to the stability of the vast majority of the mass-spectral intensity, over more than 24 h of evaporation, these changes are minor and agree qualitatively with the conclusions by Cappa and Wilson (2011).

Based on the data described so far we conclude that SOA particles are spherical, evaporate very slowly, and are highly viscous, leaving open the question whether they are rigid solids. To address this question we refine the picture by considering some additional information. The fact that the α -pinene SOA particles shown to be spherical (Vaden et al., 2010, 2011a, b; Zelenyuk et al., 2008) were generated by homogeneous nucleation followed by coagulation provides evidence that the coagulating nanoparticles could not have been rigid solids. Moreover, in our SOA aging experiments (Vaden et al., 2010), particles were characterized ~ 24 h after SOA formation. During the aging process coagulation resulted in even larger particles that were also found to be spherical, demonstrating that the phase of SOA particles does not alter significantly with time. If the coagulating SOA particles were rigid solids at any stage of their particle life cycle, one would expect aspherical agglomerates to form, which is not what we found. In addition, in Vaden et al. (2010) we showed that coating aspherical NaCl seed particles with SOA results in formation of spherical particles and that a very small fraction of the NaCl core dissolves in the SOA coating demonstrating that even when in contact with solid NaCl, SOA is not rigid solid. These observations imply that SOA particles share some properties of fluid, as they are spherical and exhibit shape-conformity to the solid NaCl core.

25 Finally, our observations of extremely slow diffusion of molecules like pyrene or DOP through SOA, provides direct evidence that SOA is highly viscous (Vaden et al., 2010, 2011a). These and more recent direct measurements of the diffusion of molecules in SOA were used to calculate the corresponding diffusivities, from which the SOA

Reformulating the atmospheric lifecycle of SOA

M. Shrivastava et al.

Title Page

Abstract

Introduction

Conclusions

References

Tables

Figures

◀

▶

◀

▶

Back

Close

Full Screen / Esc

Printer-friendly Version

Interactive Discussion



viscosity was calculated. The calculated SOA viscosity was then used to calculate particle coalescence timescales that are on the order of seconds to minutes, providing a simple explanation for the findings that the quasi-solid SOA particles are spherical and remain spherical after coagulation. Detailed calculations of diffusivity, viscosity, and coalescence timescales for SOA particles will be presented in a separate publication.

2.2 SOA evaporation

In our SOA evaporation studies (Vaden et al., (2011a) we show that pure α -pinene SOA evaporation follows a fast phase during which $\sim 40\%$ of the particle mass evaporates in ~ 2 h, followed by a slow evaporation during which additional 25% of the mass evaporates in 24 h. When α -pinene SOA is produced in the presence of hydrophobic organics, they are trapped in the SOA and their presence further slows particle evaporation. We find that this effect is further enhanced when SOA particles with trapped hydrophobic organics are aged. The evaporation of ambient SOA particles mixed with a small amount of sulfate show behavior very similar to that of laboratory generated SOA particles mixed with hydrophobic organics (Vaden et al., 2011a). These exhibit the same fast evaporation within the first ~ 100 min, which is followed by a very slow evaporation. Ambient SOA particles lose less than 20% of the particle volume in more than 4 h of evaporation under vapor-free conditions, at which point the evaporation rate is extremely slow. It is reasonable to presume that in the ambient atmosphere, where organic vapors are present, evaporation would be expected to be even slower and suggest that treating these particles as non-evaporating would be a reasonable simplifying approximation. Dilution and chemical processing of air masses reduces the concentrations of gas phase species that were at equilibrium with the SOA particles. The extremely slow SOA evaporation rates we observed imply that, in the atmosphere, reversible equilibrium between the particle and gas phase would not be maintained.

In summary: (1) SOA particles are neither liquid-like nor rigid solids; instead they are highly viscous quasi-solids. (2) SOA particles evaporate orders of magnitude slower than expected. (3) Hydrophobic organics are trapped within the SOA phase reducing

Reformulating the atmospheric lifecycle of SOA

M. Shrivastava et al.

Title Page

Abstract

Introduction

Conclusions

References

Tables

Figures

◀

▶

◀

▶

Back

Close

Full Screen / Esc

Printer-friendly Version

Interactive Discussion



SOA evaporation rate. (4) Aging SOA, especially with trapped organics, further reduces SOA evaporation rates to the point that, to first order, evaporation under ambient conditions can be ignored. (5) SOA particles are not at equilibrium with the gas-phase.

Figure 1 schematically represents the traditional picture of SOA, forming liquid-like particles that remain at equilibrium with the surrounding gas phase, and the new picture of non-evaporating, quasi-solid SOA, with trapped hydrophobic organics. This new picture casts doubt on all SOA gas-particle mass transfer calculations based on reversible partitioning and Raoult's law.

This new picture of SOA is consistent with many other field and laboratory studies (Cappa et al., 2008; Bilde and Pandis, 2001; Grieshop et al., 2007; Heald et al., 2005; Stanier et al., 2007), in which slower than expected evaporation was observed. Using tandem differential mobility analyzer (TDMA) varying flow tube temperature, Stanier et al. (2007) showed that while evaporation of single-component adipic acid aerosols compared favorably to measured vapor pressure of adipic acid, α -pinene SOA particles showed very small evaporation requiring accommodation coefficients below 0.1. Grieshop et al. (2007) measured evaporation of chamber-generated SOA using an external flow tube varying dilution ratio and concluded that evaporation is significantly slower than expected. However, insufficient residence times in the flow tube used by both Stanier et al. (2007) and Grieshop et al. (2007) (~seconds to minutes) were thought to be the reason for mass transfer limitations. Grieshop et al. (2007) also measured gas-particle partitioning of SOA at significantly longer residence times within the smog chamber itself, and found that evaporation timescales were "surprisingly slow". Cappa and Jimenez (2010) showed that 50–80% of organic aerosol measured, using the thermodenuder-aerosol mass spectrometer (TD-AMS), in Mexico City and Los Angeles would not evaporate under any atmospheric conditions.

In addition to irreversible partitioning of SOA, the new insights about the quasi-solid SOA phase indicate significant deviation from ideal-solution, suggesting a need to revise SOA formation mechanisms as well. Here we utilize the accepted lumped-component volatility basis-set (VBS) framework to form SOA (Robinson et al., 2007),

Reformulating the atmospheric lifecycle of SOA

M. Shrivastava et al.

Title Page

Abstract

Introduction

Conclusions

References

Tables

Figures

◀

▶

◀

▶

Back

Close

Full Screen / Esc

Printer-friendly Version

Interactive Discussion



but explore the use of lower activity coefficient during SOA formation to account for the highly viscous non-volatile SOA phase. We successively implement irreversible partitioning and lower activity coefficients to evaluate their effects on SOA formation and evolution, and compare the results to previous modeling approaches. In addition, we

5 explore the effect of gas-phase multi-generation fragmentation reactions on the calculated temporal evolution of the SOA mass loadings, in the reversible and irreversible partitioning approaches.

3 Reconciling SOA evaporation and growth rates

Figure 2a compares observed evaporation kinetics of laboratory α -pinene SOA and ambient SOA (Vaden et al., 2011a) against those calculated by a gas-particle kinetic mass-transfer model (Koo et al., 2003). Initial volatility distribution in the model is calculated using the 7-species VBS developed for α -pinene SOA formed by ozonolysis (Pathak et al., 2007). Details of the kinetic calculations and discussions on the use of mass accommodation coefficients (α) are presented in the supporting online text.

15 Calculations are performed for the three particle sizes (100, 151, and 251 nm) characterized in the experiments by Vaden et al. (2011a) and shown to exhibit nearly identical evaporation kinetics. Figure 2a shows that $\alpha = 1.0$ results in much faster evaporation kinetics than those measured for both laboratory and ambient SOA particles. For example, the model predicts that 151 nm particles lose 75 % of their volume in 1 min, whereas laboratory data show that it takes ~ 24 h. Figure 2a illustrates that it is possible, in the model, to slow down evaporation by lowering α from 1.0 to 0.001, at which point we calculate that 151 nm particles lose 75 % of their volume in ~ 13 h. However, reducing α to slow calculated evaporation rates also slows down SOA growth rates.

20 Figure 2b shows the results of calculations of the growth of 10 nm particles under constant concentration difference of $1 \mu\text{g m}^{-3}$ between aerosol and gas phase, and the assumption that particles are non-volatile to obtain a maximum growth rate as discussed in supporting online text. It shows that α lower than 0.1 predicts nearly no particle

Reformulating the atmospheric lifecycle of SOA

M. Shrivastava et al.

Title Page

Abstract

Introduction

Conclusions

References

Tables

Figures

◀

▶

◀

▶

Back

Close

Full Screen / Esc

Printer-friendly Version

Interactive Discussion



growth over timescales of 4 h, which is in contradiction with observed laboratory and ambient SOA formation rates (Stanier et al., 2007; Volkamer et al., 2006). Thus $\alpha \sim 1$ is needed to explain observed SOA condensation and growth, but evaporation, being kinetically inhibited requires low α values (≤ 0.001). It seems that invoking changes in the condensed phase could provide a way to reconcile the two different α 's, high α for formation with low α for evaporation. However, as expected for liquid particles, calculations for all α 's yield size-dependent evaporation kinetics, with smaller particles evaporating faster, which is in contradiction with the observed size-independent evaporation (Vaden et al., 2011a).

Figure 2a shows that under experimental conditions, with no gas phase organics present, less than 20% of ambient SOA evaporated over 4 h, suggesting that evaporation under real atmospheric conditions would be negligible. We conclude that the observed SOA evaporation behavior cannot be explained with current models that assume reversible equilibrium gas-particle partitioning behavior of liquid SOA particles, indicating a pressing need to develop a revised modeling framework that accounts for the new experimental findings.

4 Reversible vs. irreversible SOA partitioning and lower activity coefficient: box modeling examples

In this section, we present a simplified way to account for the observed irreversible partitioning of SOA, implement it in Lagrangian box model simulations, and compare the results with reversible partitioning. The box model simulates trace gas and aerosol chemistry in an air parcel, using the modified Carbon Bond Mechanism (CBM-Z) (Zaveri and Peters, 1999) with added reactions to treat condensable organic species using the VBS approach, and the MOSAIC aerosol module (Zaveri et al., 2008) with VBS treatment of SOA (Pathak et al., 2007).

Here we consider SOA formation from a single biogenic reactive organic gas (ROG), similar to α -pinene, having an OH reaction rate constant (k_{OH}) of

Reformulating the atmospheric lifecycle of SOA

M. Shrivastava et al.

Title Page

Abstract

Introduction

Conclusions

References

Tables

Figures

◀

▶

◀

▶

Back

Close

Full Screen / Esc

Printer-friendly Version

Interactive Discussion



$4 \times 10^{-11} \text{ cm}^3 \text{ molecule}^{-1} \text{ s}^{-1}$ and fixed yields to the 7-species VBS (Pathak et al., 2007). The initial ROG concentration is 10 ppb, and initial concentrations of NO_x , O_3 , and ROGs are representative of typical suburban conditions in the atmosphere. The air parcel mixes with clean background air at a dilution rate of 6.12 % per hour (Voss et al., 2010). Following one diurnal cycle, in which SOA is formed as ROG reacts with OH during the day, gas-phase chemistry is switched off and dilution reduces both gas and particle concentrations.

In the first set of simulations we compare the reversible equilibrium gas-particle partitioning modeled with 7-species VBS as described by Donahue et al. (2006), and our revised approach, in which SOA is prevented from evaporating. In the revised approach, SOA growth by condensation is modeled similar to the traditional approach and irreversible partitioning is implemented by modifying the SOA gas-particle partitioning algorithm, so that gas and particle concentrations are left unchanged when the thermodynamics favor evaporation of SOA thus preventing SOA evaporation, but gas and particle concentrations are equilibrated when thermodynamics favor condensation. Note that this allows us to use the same 7-species VBS and thermodynamic-partitioning code to model both the previous and revised approaches.

Figure 3a shows the initial gas-particle distribution, when chemistry is switched off and the SOA concentration (C_{SOA}) is $2.2 \mu\text{g m}^{-3}$. Figure 3b shows the calculated SOA enhancement ratio, defined as ratio of SOA concentration and the dilution factor (DF), after the OH concentration drops to zero. By the time the system is diluted by a factor of 10, which for a dilution rate of 6.12 % per hour is 37 h, almost all the SOA disappears by evaporation in the reversible partitioning approach, while the SOA enhancement ratio with the new, non-evaporation approach remains constant. This clearly indicates that the irreversible partitioning approach would increase modeled SOA concentrations and significantly affect calculated background loading resulting from long-range transport to cleaner environments, which would be consistent with field observations.

For example, Heald et al. (2005) found that aircraft measurements of organic carbon over the Northwest Pacific revealed little vertical gradient in the free troposphere and

Reformulating the atmospheric lifecycle of SOA

M. Shrivastava et al.

Title Page

Abstract

Introduction

Conclusions

References

Tables

Figures

◀

▶

◀

▶

Back

Close

Full Screen / Esc

Printer-friendly Version

Interactive Discussion



10–100 times higher concentrations, as compared to SOA loadings predicted from a global chemical transport model. Using the Chung and Seinfeld (2002) parameterizations, in which SOA is treated as semi-volatile, they predicted almost complete SOA evaporation for the free troposphere. The new picture we present, in which partitioning of SOA is irreversible, may partly explain the high SOA concentrations observed in the free troposphere.

So far, we looked at dilution and partitioning of SOA when gas-phase chemistry is turned off. In the actual atmosphere, dilution and chemistry occur simultaneously. Currently, most 3-D models employing the VBS parameterization assume that SOA formation occurs due to gas-phase oxidation reactions that produce lower volatility products and thereby move the SOA mass to lower volatility bins (Robinson et al., 2007; Shrivastava et al., 2008; Tsimpidi et al., 2010). In these models, as the gas-phase concentrations decrease and the condensed phase responds by evaporation, the evaporated gas reacts with OH to produce lower volatility species, in a process termed functionalization. In these models, with each generation of oxidation, the organic vapors are moved, in a stepwise fashion, to lower volatility bins, such that after a number of generations, most of the molecules condense, or conversely, the fraction of molecules in the gas phase becomes negligible and the system is protected from further loss. Because these models push the evaporating organics to extremely low vapor pressures, it would not be surprising to find that switching evaporation off would have only small effects on the total SOA formed.

However, it is well known that when OH reacts with organic molecules, a mix of products forms. Some products have lower vapor pressures, while others, produced by fragmentation reactions, are more volatile. Therefore, proper modeling of this multi-step process must include reasonable volatility distribution of higher and lower volatility products. Kroll et al. (2011) recently suggested that addition of oxygen-containing groups weakens the C-C bonds and leads to fragmentation after just 1 to 4 generations of oxidation. In that case one would expect the individual oxidation products to span a range of oxidation state, carbon number and volatility, as governed by the kinetics of

Reformulating the atmospheric lifecycle of SOA

M. Shrivastava et al.

[Title Page](#)[Abstract](#)[Introduction](#)[Conclusions](#)[References](#)[Tables](#)[Figures](#)[⏪](#)[⏩](#)[◀](#)[▶](#)[Back](#)[Close](#)[Full Screen / Esc](#)[Printer-friendly Version](#)[Interactive Discussion](#)

key organic “aging” reactions (Kroll et al., 2011).

Here we use the box model to examine SOA formation and evolution under three contrasting cases, in which reactions with OH lead primarily to functionalization (Case 1) or fragmentation (Case 2), both with activity coefficient of 1, and Case 3 that replicates Case 2, but explores the effect of lower activity coefficient. For each case, we compare reversible and irreversible partitioning. In Case 1 (Fig. 4a), 15 % of the products from each volatility species in the 7-species VBS move to the highest volatility species ($C^* = 10^4 \mu\text{g m}^{-3}$), 75 % move to the next lower volatility (e.g., from $C^* = 10^2$ to $C^* = 10 \mu\text{g m}^{-3}$), and the remaining 10 % are lost to high volatility species outside the VBS range. In Case 2 (Fig. 4b), 75 % of the products from all volatility species in the 7-species VBS move to the highest volatility species ($C^* = 10^4 \mu\text{g m}^{-3}$), 15 % move to the next lower volatility, and the remaining 10 % are lost and moved outside the VBS range. Case 3 (Fig. 4c), replicates the conditions of Case 2 with activity coefficient of 0.2. All modeling results presented in Fig. 4 include in addition to gas-phase chemistry, 6.12 % per hour dilution, with time zero corresponding to 06:00 local time (LT). Initial ROG concentrations are chosen to yield similar peak SOA concentration of about $1 \mu\text{g m}^{-3}$. Figure 4a provides comparison between the calculated temporal evolutions of SOA under assumptions of reversible and irreversible partitioning for Case 1. During the initial SOA formation period, the two partitioning approaches give nearly identical results. Once SOA concentrations peak, a small difference between the two is observed. After 24 h, the total SOA concentration from the non-evaporating approach is 20 % higher. The volatility distributions at 24 h for the two approaches (not shown) are similar, although the irreversible partitioning approach has noticeably more SOA ($C^* \geq 1 \mu\text{g m}^{-3}$). This example illustrates that when fragmentation is low and the evaporated gases react in the model to give mostly lower volatility products that re-condense, the difference between reversible and irreversible partitioning approaches is small (20 %).

Figure 4b presents the results for Case 2, where fragmentation is much greater. The SOA formation rates for the two approaches are again very close during the first few hours, later their results differ strongly. With reversible partitioning, SOA evaporates as

Reformulating the atmospheric lifecycle of SOA

M. Shrivastava et al.

Title Page

Abstract

Introduction

Conclusions

References

Tables

Figures

⏪

⏩

◀

▶

Back

Close

Full Screen / Esc

Printer-friendly Version

Interactive Discussion



the air parcel dilutes, and the resulting gas-phase species react with high probability of fragmentation to produce higher volatility species that do not re-condense. SOA evaporates much faster during the day as compared to nighttime due to fragmentation, as shown by the higher daytime slope of reversible partitioning. Figure 4b shows that in 24 h, evaporation and fragmentation reactions transfer almost all the SOA from the particle to the gas-phase. With the irreversible partitioning approach, SOA stays in the particle phase (Fig. 4b), and the SOA enhancement ratio remains constant. These results illustrate that when gas-phase chemistry favors fragmentation, stopping evaporation yields significantly more SOA, providing clear illustration of the importance of coupling evaporation with fragmentation reactions in model predicted SOA loadings, as discussed by Jimenez et al. (2009).

In both reversible and irreversible partitioning approaches, SOA formation is modeled using the VBS approach, in which vapor pressures and Raoult's law determine the condensing fraction. However, the experimentally observed SOA evaporation rates clearly show that the lumped component vapor pressures of the condensed SOA phase is much lower than that predicted by Raoult's law. Cappa et al. (2008) used a temperature programmed thermal desorption (TPTD) method and found non-ideal solution behavior with activity coefficients lower than 1 for a mixture of atmospherically relevant C3-C7 diacids. In addition, they found that the presence of inorganic salt caused further changes in desorption behavior of the organic mixture. In Vaden et al. (2011a) we showed that semi-volatile hydrophobic organic vapors, like pyrene trapped within SOA particles decrease their evaporation rates. Hence, studies by Cappa et al. (2008) and by us (Vaden et al., 2011a) suggested that complex interaction phenomena between different organic molecules and between organic and inorganic molecules changed evaporation behavior. In Fig. 4c, we explore an effect of complex molecular interactions and non-ideal SOA formation behavior, as described by Case 3 above by using activity coefficient of 0.2. It shows that for irreversible partitioning, lower activity coefficient yields 3 times as much SOA as compared to Fig. 4b. While higher non-ideal SOA forms in the reversible case as well, it is lost within 24 h due to evaporation and

Reformulating the atmospheric lifecycle of SOA

M. Shrivastava et al.

Title Page

Abstract

Introduction

Conclusions

References

Tables

Figures

◀

▶

◀

▶

Back

Close

Full Screen / Esc

Printer-friendly Version

Interactive Discussion



fragmentation reactions as shown in Fig. 4c.

5 SOA in the Mexico City region: a 3-D Modeling Example

In this section, we present a modeling example, in which the effects of irreversible partitioning and fragmentation are examined under more realistic atmospheric conditions, using WRF-Chem, a 3-D chemical transport model, that was modified to implement the 9-species VBS mechanism to simulate formation and evolution of the organic aerosols (Shrivastava et al. (2011)). The model includes SOA formed from semi-volatile and intermediate volatile precursors emitted from anthropogenic and biomass-burning sources, and traditional SOA formed from biogenic and anthropogenic ROGs. Table 1 in Shrivastava et al. (2011) provides a complete list of the terminology for various types of organic aerosol species that are included in this modeling activity.

The main difference between the present simulations and simulations presented in Shrivastava et al. (2011), is that in the previous work 100 % functionalization was assumed for all generations, and in the present study, 100 % functionalization is assumed only for the first two generations. Third generation and thereafter are assumed to undergo 75 % fragmentation, leading to formation of highest volatility species in the VBS that is still available for further functionalization and fragmentation reactions. At each step of oxidation, 10 % of each gas-phase VBS species is moved outside the VBS range and not tracked further, assuming it is eventually oxidized to CO₂. In addition, we assume that primary organic aerosols (POA) and SOA form separate organic solutions and do not mix. As a result, POA does not affect gas-particle partitioning of SOA. Reversible partitioning and activity coefficient of 1 is assumed for POA in all cases, regardless of whether partitioning of SOA is reversible or irreversible. Note that POA is left unchanged in all the simulated Cases. Initial and boundary conditions on the outer domain (far from region shown in Fig. 5) for all SOA species are assumed to be zero. However, a small amount of background organic aerosol (0.1–0.3 μg m⁻³) obtained from MOZART global simulations of trace gases and aerosols (Emmons et al.,

Reformulating the atmospheric lifecycle of SOA

M. Shrivastava et al.

Title Page

Abstract

Introduction

Conclusions

References

Tables

Figures

⏪

⏩

◀

▶

Back

Close

Full Screen / Esc

Printer-friendly Version

Interactive Discussion



2010), is allowed to form a solution with SOA.

Figure 5a and b show the calculated SOA surface concentrations over an inner nested domain, at $3 \times 3 \text{ km}^2$ grid resolution, for the reversible and irreversible approaches on 10 March 2006 at 13:30 LT, assuming activity coefficient of 1. The simulation period is 6–11 March 2006. Horizontal wind vectors averaged for six hours from 07:30 to 13:30 LT at the surface, represented by arrows, are also shown.

Comparison between the two approaches in Fig. 5a and b shows that the case, in which evaporation is stopped, the SOA plume north of the city center reaches up to $6.5 \mu\text{g m}^{-3}$, significantly higher than in the reversible partitioning case. The wide region north-east of Mexico City in Fig. 5b shows SOA concentrations $\geq 7 \mu\text{g m}^{-3}$ due to air mass transported through Mexico City region and farther south-east including Veracruz. Here as well, irreversible partitioning predicts 2.5 times higher SOA as compared to reversible partitioning case shown in Fig. 5a. Greater differences (up to a factor of 3) between the irreversible and reversible partitioning approaches are seen where SOA concentrations are lower, as dilution causes evaporation of SOA in the reversible approach.

In Fig. 5c, we show the results of simulation, in which the conditions in Fig. 5b are replicated except for the activity coefficient of 0.2, similar to our box model example above, which reduces the effective volatilities of all SOA species by a factor of 5. Not surprisingly, we find in this case that the calculated SOA concentrations near the city and in background are significantly higher than in either of the two previous cases shown in Fig. 5a and b.

6 Discussions

Recent laboratory and field data provide new important information about phase and evaporation kinetics of SOA particles in the atmosphere. When these data are considered in their entirety, a new picture of SOA emerges. The data indicate that lower volatility molecules condense to form highly viscous, quasi-solid SOA particles and do

Reformulating the atmospheric lifecycle of SOA

M. Shrivastava et al.

Title Page

Abstract

Introduction

Conclusions

References

Tables

Figures

◀

▶

◀

▶

Back

Close

Full Screen / Esc

Printer-friendly Version

Interactive Discussion



Reformulating the atmospheric lifecycle of SOA

M. Shrivastava et al.

Title Page

Abstract

Introduction

Conclusions

References

Tables

Figures

◀

▶

◀

▶

Back

Close

Full Screen / Esc

Printer-friendly Version

Interactive Discussion



not form ideal liquid-phase solution as described by Raoult's law. In addition, our data unequivocally show that SOA particles are not rigid solids. SOA particle formation and growth involve trapping of adsorbed hydrophobic organic vapors producing particles whose evaporation rates are so slow that they can be ignored. The slow evaporation rates also mean that particles are not in equilibrium with gas phase even on very long, atmospherically relevant timescales. These conclusions are in sharp contrast with some previous interpretations of similar experimental observations (Grieshop et al., 2007; Stanier et al., 2007). In our picture, SOA evolution in the atmosphere can be modeled, to a first degree, as irreversible gas-to-particle partitioning, in which the particles are not in equilibrium with the gas-phase.

Previous model parameterizations have shown reduction in model-measurement discrepancies (Dzepina et al., 2009, 2011; Hodzic et al., 2010; Robinson et al., 2007). However, significant problems and uncertainties exist in those approaches. Dzepina et al. (2011) noted that a wide diversity of SOA aging parameterizations can explain the observed regional SOA loadings measured during MILAGRO 2006. Moreover, these models assumed 100 % functionalization which led to unrealistic reductions of volatilities of all organic species, leading to artificial enhancement in predicted aerosol loadings. Also the emissions of major SOA precursors including semi-volatile and intermediate volatility organic vapors (S/IVOC) were poorly constrained, and estimated to be 6.5 times POA (Tsimpidi et al. (2010). Recently, Shrivastava et al. (2011) demonstrated the limitations in models, which led to significant bias in model-predicted SOA at both ground sites and aircraft transects as compared to measurements.

Our measurements provide the first conclusive evidence that SOA evaporation at room temperature is extremely slow even under organic-vapor-free conditions (Vaden et al., 2011a). There is a very important difference between our results and recent interpretations of ambient thermo-denuder measurements (Cappa and Jimenez, 2010), that show a large fraction of atmospheric aerosol to be non-volatile. Previous studies (e.g., Cappa and Jimenez, 2010) were interpreted to provide support for the decreased volatility of SOA with atmospheric evolution. In the previous picture, the semi-volatile

components of freshly made SOA evaporate, oxidize due to multi-generation chemistry with 100 % functionalization, and recondense due to reduction of their vapor pressure to produce very low volatility SOA (Robinson et al., 2007). In contrast, our experimental data show that the evaporation rates of even freshly made SOA are already orders of magnitude slower than expected.

Our box modeling results presented, in Sect. 4 show that irreversible partitioning yields results that are slightly higher than those obtained by traditional reversible partitioning models when both models assume 100 % functionalization (artificially pushing SOA species to lower volatility bins) as implemented by Robinson et al. (2007). The strong similarity between the two indicates that irreversible partitioning, as implemented in our revised models, are just as successful in reducing model-measurement discrepancies as models that assume 100 % functionalization, which is known to be unrealistic. Note that while irreversible partitioning approach instantaneously prevents SOA evaporation in all volatility bins, in the traditional reversible partitioning case, SOA species are efficiently moved to lower volatility bins through multiple generations of chemistry reducing their evaporation.

To examine the effect of fragmentation on the current and new formalisms we presented a simplified approach that is based on a modified VBS modeling framework. We demonstrated, for the first time, that when models take into account fragmentation reactions, irreversible gas-particle partitioning, and non-ideal SOA behavior, they predict significantly higher SOA loadings than prevailing models. In the new approach, we account, at this point, for non-ideal effects and viscous SOA phase by using lower activity coefficient, and maintain condensed SOA constituents irreversibly in the particles by stopping evaporation in models. Irreversible partitioning implies significantly increasing atmospheric SOA lifetimes and loadings as compared to previous models (Heald et al., 2005; Robinson et al., 2007). These results also imply that when experimentally observed SOA behavior is implemented in models, it would help to constrain both SOA precursor emissions and aging parameterizations significantly increasing the predictive capabilities of models representing the spatial and temporal variations of SOA in the

Reformulating the atmospheric lifecycle of SOA

M. Shrivastava et al.

Title Page

Abstract

Introduction

Conclusions

References

Tables

Figures

◀

▶

◀

▶

Back

Close

Full Screen / Esc

Printer-friendly Version

Interactive Discussion



atmosphere.

High SOA viscosity also implies changes in hygroscopic properties, cloud condensation activity, heterogeneous chemistry, and light scattering of organic aerosols affecting both aerosols and aerosol-cloud interactions. This work has important implications to understanding climate impacts of atmospheric aerosols, suggesting the need to reformulate existing aerosol models to better represent SOA behavior in the atmosphere.

Finally, we note that this paper does not claim to have developed a robust modeling framework. Instead, it uses a simplified modification to existing models to develop fundamental scientific insights on how the physical and chemical evolution of SOA in the atmosphere is affected by the new experimental findings.

Supplement related to this article is available online at:
**[http://www.atmos-chem-phys-discuss.net/11/20107/2011/
acpd-11-20107-2011-supplement.pdf](http://www.atmos-chem-phys-discuss.net/11/20107/2011/acpd-11-20107-2011-supplement.pdf)**

Acknowledgements. The authors would like to thank Evan Abramson for helpful discussions. This work was supported by the US Department of Energy Office of Biological and Environmental Research (Atmospheric Research Program) and Office of Basic Energy Sciences, Division of Chemical Sciences, Geosciences, and Biosciences. This research was performed in the Environmental Molecular Sciences Laboratory, a national scientific user facility sponsored by the Department of Energy's Office of Biological and Environmental Research at Pacific Northwest National Laboratory (PNNL). PNNL is operated by the US Department of Energy by Battelle Memorial Institute undercontract No. DE-AC0676RL0 1830.

Reformulating the atmospheric lifecycle of SOA

M. Shrivastava et al.

Title Page

Abstract

Introduction

Conclusions

References

Tables

Figures

◀

▶

◀

▶

Back

Close

Full Screen / Esc

Printer-friendly Version

Interactive Discussion



References

- Bahreini, R., Keywood, M. D., Ng, N. L., Varutbangkul, V., Gao, S., Flagan, R. C., Seinfeld, J. H., Worsnop, D. R., and Jimenez, J. L.: Measurements of secondary organic aerosol from oxidation of cycloalkenes, terpenes, and m-xylene using an Aerodyne aerosol mass spectrometer, *Environ. Sci. Technol.*, 39, 5674–5688, doi:10.1021/es048061a, 2005.
- Bilde, M. and Pandis, S. N.: Evaporation rates and vapor pressures of individual aerosol species formed in the atmospheric oxidation of alpha- and beta-pinene, *Environ. Sci. Technol.*, 35, 3344–3349, 2001.
- Cappa, C. D., Lovejoy, E. R., and Ravishankara, A. R.: Evidence for liquid-like and nonideal behavior of a mixture of organic aerosol components, *Proc. Natl. Acad. Sci. USA*, 105, 18687–18691, doi:10.1073/pnas.0802144105, 2008.
- Cappa, C. D. and Jimenez, J. L.: Quantitative estimates of the volatility of ambient organic aerosol, *Atmos. Chem. Phys.*, 10, 5409–5424, doi:10.5194/acp-10-5409-2010, 2010.
- Cappa, C. D. and Wilson, K. R.: Evolution of organic aerosol mass spectra upon heating: implications for OA phase and partitioning behavior, *Atmos. Chem. Phys.*, 11, 1895–1911, doi:10.5194/acp-11-1895-2011, 2011.
- Chung, S. H. and Seinfeld, J. H.: Global distribution and climate forcing of carbonaceous aerosols, *J. Geophys. Res.-Atmos.*, 107, 4407, doi:10.1029/2001jd001397, 2002.
- de Gouw, J. A., Middlebrook, A. M., Warneke, C., Goldan, P. D., Kuster, W. C., Roberts, J. M., Fehsenfeld, F. C., Worsnop, D. R., Canagaratna, M. R., Pszenny, A. A. P., Keene, W. C., Marchewka, M., Bertman, S. B., and Bates, T. S.: Budget of organic carbon in a polluted atmosphere: Results from the New England Air Quality Study in 2002, *J. Geophys. Res.-Atmos.*, 110, D16305, doi:10.1029/2004jd005623, 2005.
- Donahue, N. M., Robinson, A. L., Stanier, C. O., and Pandis, S. N.: Coupled partitioning, dilution, and chemical aging of semivolatile organics, *Environ. Sci. Technol.*, 40, 02635–02643, doi:10.1021/es052297c, 2006.
- Dzepina, K., Volkamer, R. M., Madronich, S., Tulet, P., Ulbrich, I. M., Zhang, Q., Cappa, C. D., Ziemann, P. J., and Jimenez, J. L.: Evaluation of recently-proposed secondary organic aerosol models for a case study in Mexico City, *Atmos. Chem. Phys.*, 9, 5681–5709, doi:10.5194/acp-9-5681-2009, 2009.
- Dzepina, K., Cappa, C. D., Volkamer, R. M., Madronich, S., DeCarlo, P. F., Zaveri, R. A., and Jimenez, J. L.: Modeling the Multiday Evolution and Aging of Secondary Organic Aerosol

Reformulating the atmospheric lifecycle of SOA

M. Shrivastava et al.

Title Page

Abstract

Introduction

Conclusions

References

Tables

Figures

◀

▶

◀

▶

Back

Close

Full Screen / Esc

Printer-friendly Version

Interactive Discussion



**Reformulating the
atmospheric lifecycle
of SOA**

M. Shrivastava et al.

Title Page

Abstract

Introduction

Conclusions

References

Tables

Figures

◀

▶

◀

▶

Back

Close

Full Screen / Esc

Printer-friendly Version

Interactive Discussion



Atmos. Chem. Phys., 10, 5491–5514, doi:10.5194/acp-10-5491-2010, 2010.

Jimenez, J. L., Canagaratna, M. R., Donahue, N. M., Prevot, A. S. H., Zhang, Q., Kroll, J. H., DeCarlo, P. F., Allan, J. D., Coe, H., Ng, N. L., Aiken, A. C., Docherty, K. S., Ulbrich, I. M., Grieshop, A. P., Robinson, A. L., Duplissy, J., Smith, J. D., Wilson, K. R., Lanz, V. A., Hueglin, C., Sun, Y. L., Tian, J., Laaksonen, A., Raatikainen, T., Rautiainen, J., Vaattovaara, P., Ehn, M., Kulmala, M., Tomlinson, J. M., Collins, D. R., Cubison, M. J., Dunlea, E. J., Huffman, J. A., Onasch, T. B., Alfarra, M. R., Williams, P. I., Bower, K., Kondo, Y., Schneider, J., Drewnick, F., Borrmann, S., Weimer, S., Demerjian, K., Salcedo, D., Cottrell, L., Griffin, R., Takami, A., Miyoshi, T., Hatakeyama, S., Shimono, A., Sun, J. Y., Zhang, Y. M., Dzepina, K., Kimmel, J. R., Sueper, D., Jayne, J. T., Herndon, S. C., Trimborn, A. M., Williams, L. R., Wood, E. C., Middlebrook, A. M., Kolb, C. E., Baltensperger, U., and Worsnop, D. R.: Evolution of Organic Aerosols in the Atmosphere, *Science*, 326, 1525–1529, doi:10.1126/science.1180353, 2009.

Koo, B. Y., Ansari, A. S., and Pandis, S. N.: Integrated approaches to modeling the organic and inorganic atmospheric aerosol components, *Atmos. Environ.*, 37, 4757–4768, doi:10.1016/j.atmosenv.2003.08.016, 2003.

Kroll, J. H. and Seinfeld, J. H.: Chemistry of secondary organic aerosol: Formation and evolution of low-volatility organics in the atmosphere, *Atmos. Environ.*, 42, 3593–3624, doi:10.1016/j.atmosenv.2008.01.003, 2008.

Kroll, J. H., Donahue, N. M., Jimenez, J. L., Kessler, S. H., Canagaratna, M. R., Wilson, K. R., Altieri, K. E., Mazzoleni, L. M., Wozniak, A. S., Bluhm, H., Mysak, E. R., Smith, J. D., Kolb, C. E., and Worsnop, D. R.: Carbon oxidation state as a metric for describing the chemistry of atmospheric organic aerosol, *Nature Chem.*, 3, 133–139, 2011.

Molina, M. J., Molina, L. T., and Kolb, C. E.: Gas-phase and heterogeneous chemical kinetics of the troposphere and stratosphere, *Annu. Rev. Phys. Chem.*, 47, 327–367, 1996.

Odum, J. R., Hoffmann, T., Bowman, F., Collins, D., Flagan, R. C., and Seinfeld, J. H.: Gas/particle partitioning and secondary organic aerosol yields, *Environ. Sci. Technol.*, 30, 2580–2585, 1996.

Pankow, J. F.: An absorption model of the gas aerosol partitioning involved in the formation of secondary organic aerosol *Atmos. Environ.*, 28, 189–193, 1994.

Pathak, R. K., Presto, A. A., Lane, T. E., Stanier, C. O., Donahue, N. M., and Pandis, S. N.: Ozonolysis of alpha-pinene: parameterization of secondary organic aerosol mass fraction, *Atmos. Chem. Phys.*, 7, 3811–3821, doi:10.5194/acp-7-3811-2007, 2007.

**Reformulating the
atmospheric lifecycle
of SOA**M. Shrivastava et al.

[Title Page](#)[Abstract](#)[Introduction](#)[Conclusions](#)[References](#)[Tables](#)[Figures](#)[◀](#)[▶](#)[◀](#)[▶](#)[Back](#)[Close](#)[Full Screen / Esc](#)[Printer-friendly Version](#)[Interactive Discussion](#)

Pfrang, C., Shiraiwa, M., and Pöschl, U.: Chemical ageing and transformation of diffusivity in semi-solid multi-component organic aerosol particles, *Atmos. Chem. Phys. Discuss.*, 11, 13003–13033, doi:10.5194/acpd-11-13003-2011, 2011.

Pöschl, U.: Atmospheric aerosols: Composition, transformation, climate and health effects, *Angew. Chem.-Int. Edit.*, 44, 7520–7540, doi:10.1002/anie.200501122, 2005.

Ravishankara, A. R.: Heterogeneous and multiphase chemistry in the troposphere, *Science*, 276, 1058–1065, 1997.

Robinson, A. L., Donahue, N. M., Shrivastava, M. K., Weitkamp, E. A., Sage, A. M., Grieshop, A. P., Lane, T. E., Pierce, J. R., and Pandis, S. N.: Rethinking organic aerosols: Semivolatile emissions and photochemical aging, *Science*, 315, 1259–1262, doi:10.1126/science.1133061, 2007.

Salcedo, D., Onasch, T. B., Dzepina, K., Canagaratna, M. R., Zhang, Q., Huffman, J. A., DeCarlo, P. F., Jayne, J. T., Mortimer, P., Worsnop, D. R., Kolb, C. E., Johnson, K. S., Zuberi, B., Marr, L. C., Volkamer, R., Molina, L. T., Molina, M. J., Cardenas, B., Bernabe, R. M., Marquez, C., Gaffney, J. S., Marley, N. A., Laskin, A., Shutthanandan, V., Xie, Y., Brune, W., Leshner, R., Shirley, T., and Jimenez, J. L.: Characterization of ambient aerosols in Mexico City during the MCMA-2003 campaign with Aerosol Mass Spectrometry: results from the CENICA Supersite, *Atmos. Chem. Phys.*, 6, 925–946, doi:10.5194/acp-6-925-2006, 2006.

Salcedo, D., Onasch, T. B., Canagaratna, M. R., Dzepina, K., Huffman, J. A., Jayne, J. T., Worsnop, D. R., Kolb, C. E., Weimer, S., Drewnick, F., Allan, J. D., Delia, A. E., and Jimenez, J. L.: Technical Note: Use of a beam width probe in an Aerosol Mass Spectrometer to monitor particle collection efficiency in the field, *Atmos. Chem. Phys.*, 7, 549–556, doi:10.5194/acp-7-549-2007, 2007.

Shrivastava, M., Fast, J., Easter, R., Gustafson Jr., W. I., Zaveri, R. A., Jimenez, J. L., Saide, P., and Hodzic, A.: Modeling organic aerosols in a megacity: comparison of simple and complex representations of the volatility basis set approach, *Atmos. Chem. Phys.*, 11, 6639–6662, doi:10.5194/acp-11-6639-2011, 2011.

Shrivastava, M. K., Lane, T. E., Donahue, N. M., Pandis, S. N., and Robinson, A. L.: Effects of gas particle partitioning and aging of primary emissions on urban and regional organic aerosol concentrations, *J. Geophys. Res.-Atmos.*, 113, D18301, doi:10.1029/2007jd009735, 2008.

Song, C., Zaveri, R. A., Alexander, M. L., Thornton, J. A., Madronich, S., Ortega, J. V., Zelenyuk, A., Yu, X. Y., Laskin, A., and Maughan, D. A.: Effect of hydrophobic primary organic aerosols

Reformulating the atmospheric lifecycle of SOA

M. Shrivastava et al.

[Title Page](#)[Abstract](#)[Introduction](#)[Conclusions](#)[References](#)[Tables](#)[Figures](#)[◀](#)[▶](#)[◀](#)[▶](#)[Back](#)[Close](#)[Full Screen / Esc](#)[Printer-friendly Version](#)[Interactive Discussion](#)

on secondary organic aerosol formation from ozonolysis of alpha-pinene, *Geophys. Res. Lett.*, 34, L20803, doi:10.1029/2007gl030720, 2007.

Stanier, C. O., Pathak, R. K., and Pandis, S. N.: Measurements of the volatility of aerosols from alpha-pinene ozonolysis, *Environ. Sci. Technol.*, 41, 2756–2763, doi:10.1021/es0519280, 2007.

Tsimpidi, A. P., Karydis, V. A., Zavala, M., Lei, W., Molina, L., Ulbrich, I. M., Jimenez, J. L., and Pandis, S. N.: Evaluation of the volatility basis-set approach for the simulation of organic aerosol formation in the Mexico City metropolitan area, *Atmos. Chem. Phys.*, 10, 525–546, doi:10.5194/acp-10-525-2010, 2010.

Vaden, T. D., Song, C., Zaveri, R. A., Imre, D., and Zelenyuk, A.: Morphology of mixed primary and secondary organic particles and the adsorption of spectator organic gases during aerosol formation, *Proc. Natl. Acad. Sci. U. S. A.*, 107, 6658–6663, doi:10.1073/pnas.0911206107, 2010.

Vaden, T. D., Imre, D., Beranek, J., Shrivastava, M., and Zelenyuk, A.: Evaporation kinetics and phase of laboratory and ambient secondary organic aerosol, *Proc. Natl. Acad. Sci. USA*, 108(6), 2190–2195, doi:10.1073/pnas.1013391108, 2011a.

Vaden, T. D., Imre, D., Beranek, J., and Zelenyuk, A.: Extending the Capabilities of Single Particle Mass Spectrometry: I. Measurements of Aerosol Number Concentration, Size Distribution, and Asphericity, *Aerosol Sci. Technol.*, 45, 113–124, doi:10.1080/02786826.2010.526155, 2011b.

Virtanen, A., Joutsensaari, J., Koop, T., Kannosto, J., Yli-Pirila, P., Leskinen, J., Makela, J. M., Holopainen, J. K., Poschl, U., Kulmala, M., Worsnop, D. R., and Laaksonen, A.: An amorphous solid state of biogenic secondary organic aerosol particles, *Nature*, 467, 824–827, doi:10.1038/nature09455, 2010.

Volkamer, R., Jimenez, J. L., San Martini, F., Dzepina, K., Zhang, Q., Salcedo, D., Molina, L. T., Worsnop, D. R., and Molina, M. J.: Secondary organic aerosol formation from anthropogenic air pollution: Rapid and higher than expected, *Geophys. Res. Lett.*, 33, L17811, doi:10.1029/2006gl026899, 2006.

Voss, P. B., Zaveri, R. A., Flocke, F. M., Mao, H., Hartley, T. P., DeAmicis, P., Deonandan, I., Contreras-Jimenez, G., Martinez-Antonio, O., Estrada, M. F., Greenberg, D., Campos, T. L., Weinheimer, A. J., Knapp, D. J., Montzka, D. D., Crouse, J. D., Wennberg, P. O., Apel, E., Madronich, S., and de Foy, B.: Long-range pollution transport during the MILAGRO-2006 campaign: a case study of a major Mexico City outflow event using free-floating altitude-

controlled balloons, *Atmos. Chem. Phys.*, 10, 7137–7159, doi:10.5194/acp-10-7137-2010, 2010.

Zaveri, R. A. and Peters, L. K.: A new lumped structure photochemical mechanism for large-scale applications, *J. Geophys. Res.-Atmos.*, 104, 30387–30415, 1999.

5 Zaveri, R. A., Easter, R. C., Fast, J. D., and Peters, L. K.: Model for Simulating Aerosol Interactions and Chemistry (MOSAIC), *J. Geophys. Res.-Atmos.*, 113, D13204, doi:10.1029/2007jd008782, 2008.

10 Zelenyuk, A., Yang, J., Song, C., Zaveri, R. A., and Imre, D.: A New Real-Time Method for Determining Particles' Sphericity and Density: Application to Secondary Organic Aerosol Formed by Ozonolysis of alpha-Pinene, *Environ. Sci. Technol.*, 42, 8033–8038, doi:10.1021/es8013562, 2008.

15 Zelenyuk, A., Ezell, M. J., Perraud, V., Johnson, S. N., Bruns, E. A., Yu, Y., Imre, D., Alexander, M. L., and Finlayson-Pitts, B. J.: Characterization of organic coatings on hygroscopic salt particles and their atmospheric impacts, *Atmos. Environ.*, 44, 1209–1218, doi:10.1016/j.atmosenv.2009.11.047, 2010.

20 Zhang, Q., Jimenez, J. L., Canagaratna, M. R., Allan, J. D., Coe, H., Ulbrich, I., Alfarra, M. R., Takami, A., Middlebrook, A. M., Sun, Y. L., Dzepina, K., Dunlea, E., Docherty, K., DeCarlo, P. F., Salcedo, D., Onasch, T., Jayne, J. T., Miyoshi, T., Shimonono, A., Hatakeyama, S., Takegawa, N., Kondo, Y., Schneider, J., Drewnick, F., Borrmann, S., Weimer, S., Demerjian, K., Williams, P., Bower, K., Bahreini, R., Cottrell, L., Griffin, R. J., Rautiainen, J., Sun, J. Y., Zhang, Y. M., and Worsnop, D. R.: Ubiquity and dominance of oxygenated species in organic aerosols in anthropogenically-influenced Northern Hemisphere midlatitudes, *Geophys. Res. Lett.*, 34, L13801, doi:10.1029/2007gl029979, 2007.

ACPD

11, 20107–20139, 2011

Reformulating the atmospheric lifecycle of SOA

M. Shrivastava et al.

Title Page

Abstract

Introduction

Conclusions

References

Tables

Figures

◀

▶

◀

▶

Back

Close

Full Screen / Esc

Printer-friendly Version

Interactive Discussion



Reformulating the atmospheric lifecycle of SOA

M. Shrivastava et al.

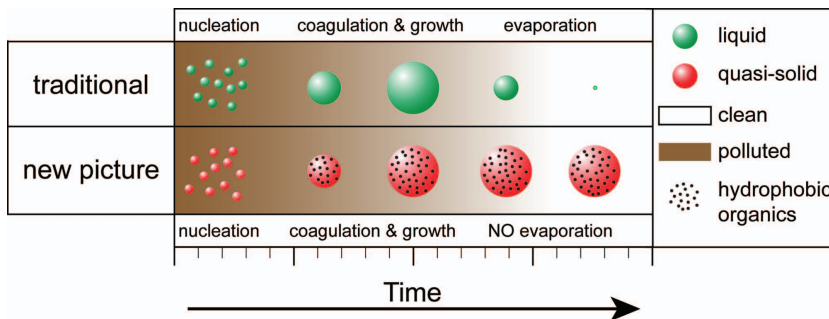


Fig. 1. Comparison of the traditional and the new picture of the SOA lifecycle in the atmosphere. In the old picture, SOA is in a liquid phase at equilibrium with the gas-phase. In the new picture, SOA is in highly viscous, quasi-solid phase; it traps hydrophobic organics, and does not evaporate on atmospherically relevant timescale.

Title Page

Abstract Introduction

Conclusions References

Tables Figures

◀ ▶

◀ ▶

Back Close

Full Screen / Esc

Printer-friendly Version

Interactive Discussion



Reformulating the atmospheric lifecycle of SOA

M. Shrivastava et al.

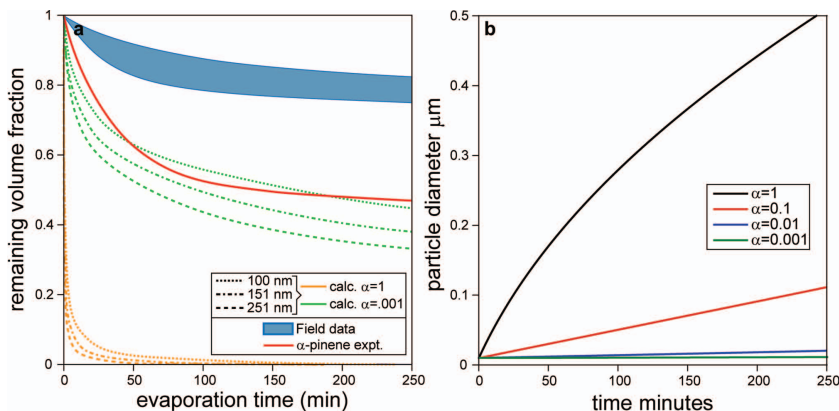


Fig. 2. (a) Comparison of measured evaporation rates of laboratory and ambient SOA particles with theoretical calculations for accommodation coefficients $\alpha = 1$ and $\alpha = 0.001$. (b) Prediction of growth rate of SOA particles with initial diameter of 10 nm for $\alpha = 1$ to $\alpha = 0.001$. Details of calculations are described in the supporting online text.

Title Page

Abstract

Introduction

Conclusions

References

Tables

Figures

◀

▶

◀

▶

Back

Close

Full Screen / Esc

Printer-friendly Version

Interactive Discussion



Reformulating the atmospheric lifecycle of SOA

M. Shrivastava et al.

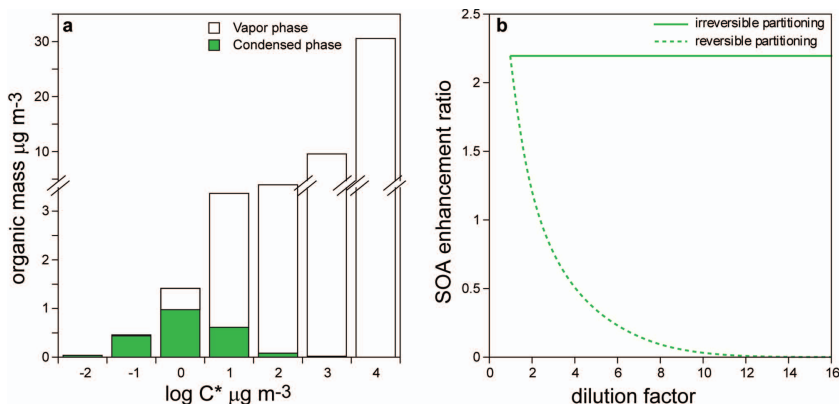


Fig. 3. Comparison between the evaporation behaviors of SOA particles in response to dilution using the traditional, reversible gas-particle partitioning, and the new, irreversible SOA condensation. **(a)** Initial gas-particle distribution denoted by 7-species VBS. **(b)** Evolution of SOA enhancement ratio as a function of dilution factor.

Reformulating the atmospheric lifecycle of SOA

M. Shrivastava et al.

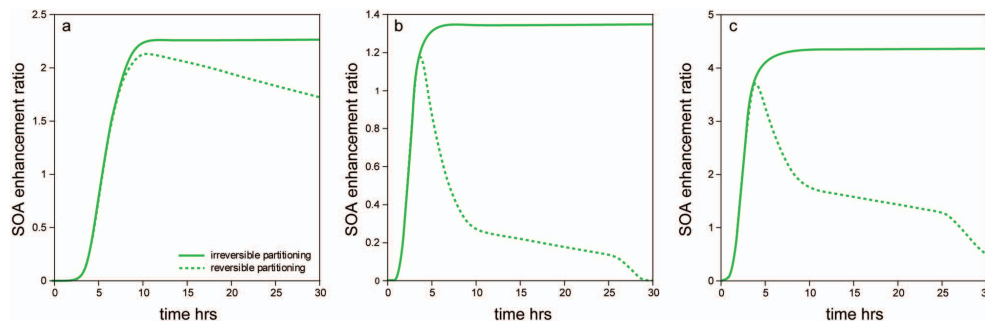


Fig. 4. Box model calculations showing the temporal evolution of the calculated SOA enhancement ratio due to functionalization, fragmentation, and dilution with multi-generational OH chemistry. **(a)** Case 1 with low fragmentation; **(b)** Case 2 with high fragmentation; **(c)** Case 3 with high fragmentation and activity coefficient of 0.2.

[Title Page](#)[Abstract](#)[Introduction](#)[Conclusions](#)[References](#)[Tables](#)[Figures](#)[◀](#)[▶](#)[◀](#)[▶](#)[Back](#)[Close](#)[Full Screen / Esc](#)[Printer-friendly Version](#)[Interactive Discussion](#)

Reformulating the atmospheric lifecycle of SOA

M. Shrivastava et al.

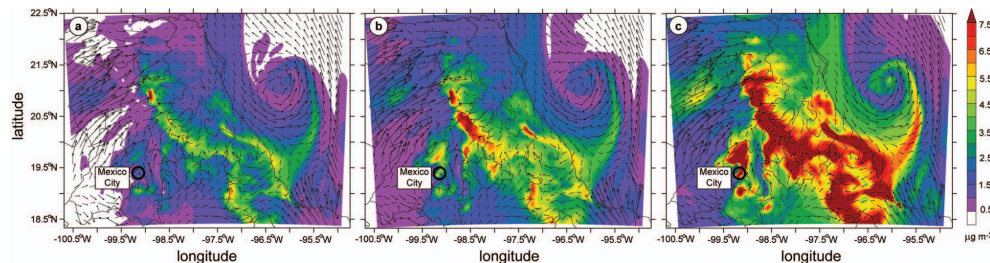


Fig. 5. WRF-Chem calculated SOA mass loadings, in the Mexico City plateau, on 10 March 2006 at 13:30 LT near the surface. **(a)** Reversible partitioning approach **(b)** Irreversible partitioning approach, with no evaporation. **(c)** Irreversible partitioning approach, with no evaporation and activity coefficient of 0.2. Mexico City is marked on the maps by a black circle. Arrows denote direction of horizontal wind vectors (07:30–13:30 LT), and length of arrows denotes magnitude of wind speed (maximum 8 m s^{-1}).

[Title Page](#)[Abstract](#)[Introduction](#)[Conclusions](#)[References](#)[Tables](#)[Figures](#)[◀](#)[▶](#)[◀](#)[▶](#)[Back](#)[Close](#)[Full Screen / Esc](#)[Printer-friendly Version](#)[Interactive Discussion](#)